A Differentiation Account of Recognition Memory: Evidence from fMRI

Amy H. Criss[1]*, Mark E. Wheeler[2]*, and James L. McClelland[3]

Abstract

■ Differentiation models of recognition memory predict a strength-based mirror effect in the distributions of subjective memory strength. Subjective memory strength should increase for targets and simultaneously decrease for foils following a strongly encoded list compared with a weakly encoded list. An alternative explanation for the strength-based mirror effect is that participants adopt a stricter criterion following a strong list than a weak list. Behavioral experiments support the differentiation account. The purpose of this study was to identify the neural bases for these differences. Encoding strength was manipulated (strong, weak) in a rapid event-related fMRI paradigm. To investigate the effect of retrieval context on foils, foils were presented in test blocks containing strong or weak targets. Imaging analyses identified regions in which activity increased faster for foils tested after a strong list than a weak list. The results are interpreted in support of a differentiation account of memory and are suggestive that the angular gyrus plays a role in evaluating evidence related to the memory decision, even for new items. ■

INTRODUCTION

Episodic memory is the ability to mentally time travel to a past experience. One method for testing episodic memory is a recognition task where participants are asked to endorse targets that were studied and reject foils that were not. Memory has been extensively studied with imaging and computational modeling techniques. However, research connecting the two fields is slim (cf, Norman & O'Reilly, 2003). Our goal is to initiate a framework for combining behavioral analysis, imaging, and modeling to understand the role of strength in recognition.

Models of memory have successfully accounted for many details of performance (see Malmberg, 2008). One exception is the role of list strength. When strength is manipulated between lists, the result is a strength-based mirror effect (SBME; Stretch & Wixted, 1998). Hit rates (HR) are higher and false alarm rates (FAR) are lower for a strongly encoded list compared with a weakly encoded list and typically the HR differences are larger than the FAR differences. Higher HRs for a strongly encoded list are predicted by all models of memory. A challenge to many models, however, is posed by the finding that the FAR differs between the strong and weak lists. Foils are drawn from the same set of items and are randomly placed into a test list following weak or strong encoding. There is no objective difference between foils tested after a weakly versus a strongly encoded list other than the encoding conditions of the target items. The criterion shift and dif-

ferentiation assumptions have been offered as competing accounts for the SBME.
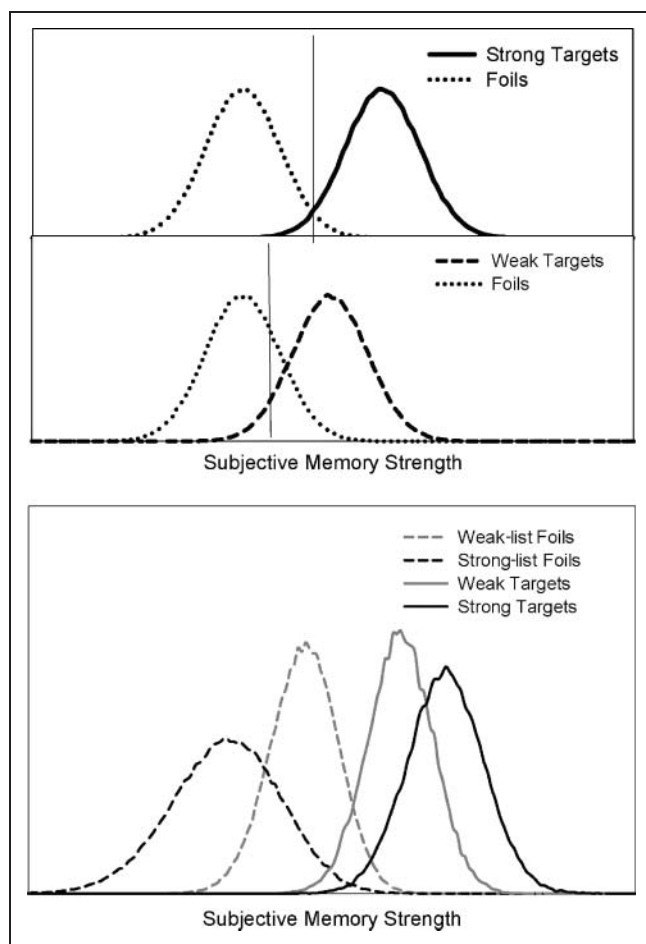
The Criterion Shift Assumption

One assumption is meta-cognitive; participants become aware that accuracy for a strong list is high, during encoding or the initial test trials, and consequently adopt a strict criterion. The reduction in FAR for a strong relative to a weak study list is accounted for by a change in the criterion. This assumption is prominent in the class of models that assumes the subjective memory strength of unrelated foils is not affected by encoding strength, as shown in Figure 1 (top). Dual process models assume two different sources on which to base the memory decision (e.g., recollecting the specific details of the event or an overall feeling of familiarity absent the details) whereas single process models assume just one basis for memory decisions. The criterion shift hypothesis has been used in both types of models, with the change in criterion affecting familiarity-based decisions (Cary & Reder, 2003; Stretch & Wixted, 1998). Critically, these models assume that the memorial evidence that a foil is from the study list (e.g., subjective memory strength) does not differ for strong-list and weak-list foils.

Differentiation Models

In differentiation models, foils following a weakly and a strongly encoded list differ in their distributions of subjective memory strength. Such models need not assume a change in the criterion to account for the SBME (see

[1]Syracuse University, [2]University of Pittsburgh, [3]Stanford University
*A. H. C. and M. E. W. contributed equally to this article.

Figure 1. Distributions of memory strength illustrating a criterion shift account of the SBME (top). The vertical line represents the criterion placement. Distributions generated from a differentiation model showing that the memory strength of targets and foils differs for strong and weak lists (bottom).

Figure 1, bottom; Criss & McClelland, 2006; McClelland & Chappell, 1998; Shiffrin & Steyvers, 1997). Differentiation models assume that better encoding of target items results in more accurate memory traces. The more accurate a given memory trace, the less likely it is that it will match a foil decreasing the FAR. In other words, the more that is known about an item, the less confusable that item is with other items. This assumption causes the distribution of subjective memory strength to increase for targets and simultaneously decrease for foils tested after a strong list compared with a weak list (see Criss, 2006, 2009, 2010). Like all memory models, differentiation models do include a criterion that can be used strategically. For example, the criterion is changed in response to the proportion of targets on the test list (e.g., Criss, 2009). In this sense the differentiation hypothesis is more robust whereas the criterion placement hypothesis can be refuted either by no evidence of a criterion shift or by evidence for differentiation. For the present purposes, the critical point made by differentiation models is that the criterion does not play a causal role in the SBME.

Whether strengthening items on a list results in a change in the memory distribution for foils and targets or a change in criterion placement is an important theoretical question. Discriminating between a differentiation account and criterion shift account of the SBME with only HRs and FARs is impossible because the signal detection parameters are saturated (four data points and four critical parameters). Evidence for differentiation models is accumulating with studies using more informative dependent measures. For example, direct ratings of subjective memory strength support a priori predictions of differentiation models. That is, participant-generated distributions of memory strength following a strong and a weak list differ as predicted by differentiation models. Critically, these participant-generated distributions of memory strength do not change with differences in target probability, a classic response bias manipulation (Criss, 2009).

Analysis of RT distributions within the diffusion model framework (e.g., Ratcliff, 1978) support differentiation models (cf, Starns, White, & Ratcliff, 2010). The diffusion model describes how information is accumulated to reach a decision. The better the quality of evidence provided by the stimulus or the decision-maker, the faster the rate of evidence accumulation, called the drift rate. In recognition memory, drift rate maps onto subjective memory strength (Ratcliff, 1978), thus differences in drift rate were predicted for strong-list foils and weak-list foils. Empirical distributions of RT were best fit by differences in the rate of evidence accumulation (e.g., drift rate) for strong and weak targets and strong-list and weak-list foils, with larger magnitudes of drift rates for targets and foils from the strong list (Criss, 2010). The magnitude of the strength differences and corresponding changes in drift rate need not be and was not identical for targets and foils. In contrast, manipulating criterion by changing the percentage of targets at test resulted in a different pattern of RT distributions that was best accounted for by changes in the starting point of the evidence accumulation process, not drift rate (Criss, 2010).

Despite a considerable body of data, described above, supporting predictions of differentiation models, it may be possible to account for the same findings within a criterion shift account. For this reason, we explored the possibility that evidence from functional imaging studies could provide additional evidence about the two accounts. The critical question in the debate between criterion shift and differentiation accounts of list strength is whether a change in response bias or memory strength is necessary for the changes in the FAR. We attempt to answer that question by comparing strong versus weak conditions within brain regions where activation is related to memory strength or response bias.

Neural Correlates of Memory Strength and Response Bias

The neural correlates of episodic memory have been well documented (for reviews, see Wagner, Shannon, Kahn, & Buckner, 2005; Buckner & Wheeler, 2001). A collection

of retrieval success areas (RSA) consistently show differential activation when hits are contrasted with correct rejections (CRs) in recognition memory tasks. RSA include inferior and superior parietal cortex, prefrontal cortex, precuneus, and cingulate gyrus (Simons et al., 2008; Wheeler & Buckner, 2004; Konishi, Wheeler, Donaldson, & Buckner, 2000; McDermott, Jones, Petersen, Lageman, & Roediger, 2000; Henson, Rugg, Shallice, Josephs, & Dolan, 1999).

Very few studies of RSA have explicitly differentiated between the contribution of memory strength and response bias to memory performance and the resulting neural activation in these areas. Many studies have shown that some RSA track factors related to memory strength. For example, regions in or near the left intraparietal sulcus are modulated by the subjective memory decision (e.g., differential activity to false alarms vs. misses; Kahn, Davachi, & Wagner, 2004; Wheeler & Buckner, 2003) and left lateral parietal regions near the angular gyrus (AG) are modulated by whether the response is recollection or familiarity based (Vilberg & Rugg, 2008; Wheeler & Buckner, 2004; Henson et al., 1999). Using subjective ratings of strength, other studies have found a set of regions in which activity correlates positively with memory strength, including left lateral parietal and inferior frontal cortex, left thalamus, and bilateral medial parietal cortex (Montaldi, Spencer, Roberts, & Mayes, 2006; Yonelinas, Otten, Shaw, & Rugg, 2005). Relatively few studies have evaluated the role of RSA in response bias manipulations. Herron, Henson, and Rugg (2004) manipulated the percentage of test items that were targets and found that, as the ratio of old to new items decreased, the difference in Hit and CR activation increased in left superior parietal, left inferior frontal, and bilateral anterior frontal regions.

O'Connor, Han, and Dobbins (2010) found correlations between signal detection measures of memory strength (d') and response bias (c) with the contrast of Hit–CR across many frontal and parietal regions including several RSA. Like O'Connor et al., we differentiate between those RSA that are modulated by response bias (RSA_c) and those RSA modulated by accuracy ($RSA_{d'}$).

Predictions

The goal of this study was to evaluate whether a criterion shift or differentiation causes list strength effects for FARs. Responses to targets as a function of list strength are less informative because both accounts predict an increase in HRs with list strength. The theories differ in their predictions for the memory strength of foils: Differentiation models predict that the memory strength of foils decreases as strength of targets increase and criterion shift models do not. We therefore focus our analyses on differences in activations produced by foils at different levels of list strength. We first identify retrieval success regions and determine whether those areas are correlated with d', and therefore considered candidate memory strength areas or are correlated with c, and therefore considered candidate response

bias areas. Such areas are designated $RSA_{d'}$ and RSA_c, respectively. We then compare strong-list foils and weak-list foils within the RSA_c and $RSA_{d'}$ to evaluate whether criterion shift or differentiation accounts best describe the processes underlying the SBME. If a criterion shift underlies list strength effects, then we should see greater activity for strong list foil trials than weak-list foil trials in RSA_c (reflecting a list-wide shift in the decision process).

If differentiation underlies list strength effects, we should see differences between strong-list and weak-list foils in regions sensitive to memory strength. However, there are two alternative ways of thinking of how these differences will be manifest. One possibility is that RSA represent the strength of memory activation. In this case, illustrated in Figure 1, strong-list foils should produce even less activation than weak-list foils in these areas. Another possibility and the one that is our primary focus here is that these areas should be thought of as associated with accumulation of evidence toward either of the two possible responses. Strong-list foils lead to faster accumulation of evidence toward the "new' response than weak-list foils. Thus, if RSA contain accumulators of evidence, we would expect to see a faster change of activation in these areas to strong-list foils than to weak-list foils (consistent with the Criss, 2010, application of the diffusion model to the SBME), especially in the most confident responses that represent the extreme edges of the memory strength distributions.

The neural correlates of information accumulation have been well documented in nonhuman primates and include FEFs, lateral intraparietal area, superior colliculus, and dorsolateral pFC (Gold & Shadlen, 2007; Schall, 2001). Relatively less research has evaluated the neural substrates associated with evidence accumulation in humans. Ho, Brown, and Serences (2009) identified a subregion of the right insula whose activity is consistent with a modality-independent evidence accumulator. In another case, Ploran et al. (2007) controlled the amount of information provided by the stimulus as a means of manipulating information accumulation. Information accumulation regions were defined as those that became active immediately following onset of the stimulus (e.g., early in the time course) and whose subsequent rate of increase in activity was related to the time taken to identify the stimulus. The rise in activity was steep for easy stimuli (identified early) and gradually decreased with stimulus difficulty. We are not aware of any studies that have evaluated the neural correlates of information accumulation in memory. Our focus builds on the rationale of Ploran et al. (2007), leading us to compare the rate of information accumulation in strong-list versus weak-list foils; however, we also consider alternatives.

METHODS

Participants

Twenty-nine right-handed native English-speaking volunteers with normal or corrected-to-normal vision participated

in the study. Data from six participants were discarded: three for chance level performance, two for insufficient numbers of observations in some conditions, and one for excessive head motion. Of the remaining 23 participants, 15 were women. Participants ranged in age from 21 to 29 ($M = 21.9$). Participants gave informed consent as required by the institutional review board of the University of Pittsburgh and were paid $25/hr for participation.

Stimuli

The word pool consisted of 700 words between 4 and 14 letters in length with a log frequency range between 8 and 14 ($M = 10.483$) among approximately 131 million words in the corpus (Balota et al., 2007).

Behavioral Paradigm

Studies focused on the cause of the SBME typically manipulate strength via repetition, and we follow that tradition here (though deep vs. shallow encoding may also produce an SBME). Critically, the mechanisms underlying recognition models operate in the same way whether information is strengthened via encoding task or repetition (e.g., Shiffrin, Ratcliff, & Clark, 1990).

At study, participants received a weak and a strong block, order counterbalanced. Each study list consisted of 100 unique words. For the weak lists, study words were presented a single time for 1.5 sec with a 500-msec ISI. For the strong lists, study words were presented for five such presentations and the entire set of 100 words was randomly ordered anew and presented before any word repeated (equating study test lag for the most recent presentation of weak and strong targets). The test list began immediately after the study list with 100 targets and 100 foils each presented for 750 msec followed by a 2250 msec ISI. Participants responded to the question "was this word on the list you just studied?" on a 4-point scale (*sure yes*, *maybe yes*, *maybe no*, *sure no*). The test trials were intermixed with 100 fixation trials, also 3 sec in duration. Order of the test trials was generated using the Buracas and Boynton (2002) method.

Image Acquisition

Images were acquired on a 3-T Siemens (Malvern, PA) MAGNETOM Allegra system at the University of Pittsburgh's Brain Imaging Research Center. Before functional imaging, a T1-weighted high-resolution magnetization prepared rapid gradient-echo image (192 parasagittal slices, 1 mm^3 voxels, repetition time = 1540 msec, echo time = 3.04 msec, flip angle = 8°, inversion time = 800 msec) was acquired. Functional images were collected during task performance using a T2*-weighted echo-planar pulse sequence sensitive to BOLD contrast (Kwong et al., 1992; Ogawa et al., 1992; repetition time = 1500 msec, echo time = 25 msec, flip angle = 79°, in-plane resolution = 3.2 ×

3.2 mm, slice thickness = 3.5 mm, 35 slices, interleaved acquisition). The first five image acquisitions per run were discarded to allow net magnetization to reach a steady state.

Procedure

The entire experiment was conducted inside the scanner; however, functional images were only collected during the test blocks. Participants were fully informed about the experimental design before entering the scanner. A brief practice block preceded the experimental blocks. Responses were collected with a glove on each hand. Index fingers corresponded to "sure" and middle fingers corresponded to "maybe." The hand used to respond yes or no was counterbalanced across subjects. Participants were asked to respond as quickly as possible without sacrificing accuracy. The experiment was conducted using E-prime (Psychology Tools, Inc., Pittsburgh, PA) and stimuli were projected from the rear of the scanner to a mirror positioned above the participants' eyes. Analysis of ROI-based data was conducted using JMP software (Version 8, SAS Institute, Inc., Cary, NC).

Functional MRI Data Analysis

Functional data were corrected for slice timing differences using sinc interpolation, realigning all slices to the first slice. Head motion was corrected within and across runs using a rigid body algorithm with three translational and three rotational parameters (Snyder, 1996). Whole-brain adjustment normalized the modal voxel value for all participants to a value of 1000 to facilitate comparison between data sets (Ojemann et al., 1997).

After preprocessing, functional data from each participant were analyzed on a voxel-by-voxel basis using a general linear model (GLM) approach (Ollinger, Shulman, & Corbetta, 2001; Miezin, Maccotta, Ollinger, Petersen, & Buckner, 2000; Friston, Jezzard, & Turner, 1994). The BOLD data in each voxel were modeled as the sum of coded effects at each time point, produced by modeled events and by unexplained variance. Event regressors were coded into each model at trial onset according to list strength (strong, weak), item type (target, foil), and accuracy (correct, incorrect). Events were modeled over 12 time points beginning at trial onset, producing a time course of BOLD activity for each event spanning 18 sec. Linear trend and constant regressors were included for each run. A series of delta functions described event-related effects as estimates of the percent signal change from the baseline term. This approach makes no assumptions about the shape of the BOLD response. Image processing and analyses were conducted using software developed at Washington University (Ollinger et al., 2001).

To identify RSA, an ANOVA was conducted using GLM parameter estimates from each participant, with Subject

treated as a random factor and Time (each whole-brain volume) as a repeated measure. A voxelwise mixed effects repeated-measures ANOVA, with fixed factors of Strength (strong, weak), Item Type (target, foil) and Time (12 time points), was computed on correct trials, collapsing over confidence response. This analysis produced a set of main effect and interaction images, one for each term in the ANOVA model. The interaction image of Item Type (correct target vs. correct foil) × Time was used to define retrieval success ROIs. This image displays the degree to which activity on correct target trials differs from activity on correct foil trials across the 12 modeled time points.

During group analyses, BOLD data were resampled into 2-mm isotropic voxels and transformed into stereotaxic atlas space by aligning an individual participant's T1-weighted image to a Talairach atlas-transformed T1-weighted template using a series of affine transformations (Fox, Snyder, Barch, Gusnard, & Raichle, 2005; Michelon, Snyder, Buckner, McAvoy, & Zacks, 2003; Lancaster et al., 1995; Talairach & Tournoux, 1988). The ANOVA produced an F-to-z-transformed statistical image, smoothed using a 6-mm FWHM Gaussian kernel, for each term in the ANOVA. These uncorrected images were then corrected for multiple comparisons and sphericity. Criteria for multiple comparison corrections were based on Monte Carlo simulations (McAvoy, Ollinger, & Buckner, 2001), with a cluster-size Type I error rate of $p < .05$ at a 70 voxel extent. Although all reported data are from voxels meeting correction criteria, both corrected and uncorrected images were retained for use in the ROI definition procedure (described in the next section). Some activations and ROIs are displayed on cortical surface representations using Caret software (Van Essen et al., 2001) using the population-average, landmark, and surface-based atlas (Van Essen, 2005).

Region Definition Procedures

To define ROIs, uncorrected smoothed group z statistical images were resmoothed using a 4-mm hard sphere kernel to reduce the number of peaks in the volume. An algorithm searched for the location of signal change peaks exceeding $p < .001$ significance, and ROI volumes were grown up to a maximum 10 mm radius of contiguous voxels around the peak coordinates, including only voxels passing threshold. Peaks separated by <10 mm were consolidated by averaging their xyz coordinates. Voxels failing to pass the sphericity and multiple comparisons corrections described in the previous section were then excluded from the ROIs. Using this approach, only corrected voxels were retained in the ROIs.

Correlational Analyses of fMRI and Behavioral Measures

The relationship between memory performance and retrieval success activity was assessed by determining the degree to which a participant's d' and c statistics correlated with an estimate of the retrieval success effect (RSE), the difference in peak activity on Hit and CR trials (O'Connor et al., 2010). To compute peak activity in each ROI, the magnitude of the BOLD response on correct target and foil trials was averaged over Time Points 4, 5, and 6 (4.5, 6.0, and 7.5 sec from trial onset). This range of time points was selected because it includes the peak time points in most regions. We note that retrieval success has been characterized both by an interaction of Item Type and Time (in Functional MRI Data Analysis section) and by differences in peak activity between correct target and foil trials (this section). The two approaches should have high agreement because most of the time the interaction of item type with time was significant due to differences at peak. This was verified by evaluating Hit–CR differences at the peak of the time course (defined as Time Points 4, 5, and 6) in each ROI (listed in Table 3). We conducted a 2 × 2 ANOVA with factors of Item Type (target, foil) and Strength (strong, weak). The main effect of Item Type was significant ($p < .05$) in all ROIs except ROI 8, left thalamus, $F(1, 22) = 2.89$, $p = .09$, no corrections for multiple comparisons.

The ROI analysis was followed by an exploratory voxelwise analysis in which correct target and foil time series were convolved with a gamma function. This approach was chosen because it provided increased power, helpful in voxelwise analyses, relative to the time-course-based analysis used in the ROI analysis. The scale parameter (β) was regressed against d' and c in two separate analyses. Images were smoothed using a 4-mm FWHM Gaussian smoothing kernel. The resulting statistical maps were corrected for multiple comparisons as described in the previous section, with a cluster size threshold of 100 voxels and Type I error rate of $p < .05$ (McAvoy et al., 2001).

RESULTS

Behavioral Results

As shown in Table 1, we find an SBME as expected. One-tailed paired t tests showed that HRs were higher for strong than weak targets, $t(22) = 8.74$, $p < .001$. FARs were numerically smaller for strong-list than weak-list foils, but the magnitude failed to reach significance, $t(22) = 1.200$, $p = .122$. The power to detect significant changes in behavior is relatively low given the small number of participants. We collected pilot data in the behavioral paradigm in which 18 volunteers participated in the exact behavioral paradigm used in the scanner including fixation trials. The combined data (excluding 1 pilot participant whose performance was at chance) show an SBME: Strong HRs are higher than weak HRs, $t(39) = 9.39$, $p < .001$, and strong-list FARs are lower than weak-list FARs, $t(39) = 2.47$, $p = .009$. For comparison with neural activation

Table 1. The Probability of Calling a Test Item Old as a Function of Type of Test Item and List Strength

fMRI Subjects	Strong	Weak	Pilot and fMRI Participants	Strong	Weak
Targets	.775 (.026)	.609 (.031)	Targets	.795 (.019)	.603 (.026)
Foils	.350 (.036)	.390 (.031)	Foils	.310 (.032)	.377 (.027)

times and for archival purposes, median RT is included in Table 2.

Imaging Results

Retrieval Success

The retrieval success analysis revealed reliably different Hit versus CR activity in or near bilateral middle frontal gyrus (MFG) and the left posterior cingulate gyrus, AG, thalamus (thal), and precuneus (Table 3 and Figure 2). These locations are consistent with commonly reported RSA (Simons et al., 2008; Vilberg & Rugg, 2008; Wagner et al., 2005; Buckner & Wheeler, 2001). To investigate the nature of the RSEs, ROIs were defined from the corrected retrieval success statistical map (see Methods) and activity on strong-list and weak-list target and foil trials, averaging over levels of confidence, was evaluated in each ROI. The time course of the BOLD response from four regions are displayed in Figure 3. Consistent with prior reports (Nelson et al., 2010; Wheeler & Buckner, 2004), activity in the AG ROI (Figure 3D) displayed a decrease relative to the GLM baseline term, with a greater magnitude of decrease on foil than target trials (Figure 3D). Whereas activity in retrieval success ROIs is often greater on target than on foil trials, activity in four of the retrieval success ROIs showed the reverse pattern. These regions were located in or near bilateral MFG (Table 3, Nos. 3, 5, and 6) and left precuneus (Table 3, No. 7). This pattern of activation may reflect facilitation in processing related to prior exposure of the targets (e.g., Grill-Spector, Henson, & Martin, 2006).

Identifying RSA_c and RSA_d'

To identify memory strength and response bias components, the peak activity on Hit minus peak activity on CR trials was computed for each participant. For each participant, this value was correlated with two measures of

Table 2. Median RT in Milliseconds for Each Condition and Each Response Type

	"Old"		"New"	
	Strong	Weak	Strong	Weak
Targets	527	705	975	837
Foils	903.5	828.5	797.5	796

behavioral performance, bias (c) to identify RSA_c and sensitivity (d') to identify $RSA_{d'}$. Strong and weak trials were analyzed separately. R values for each ROI for strong and weak conditions are listed in Table 3.

This analysis identified correlations of the RSE with c in both left MFG ROIs in the strong condition only ($R = .47$, $p = .02$ and $R = .42$, $p = .04$). RSE did not correlate with d' for the strong condition in either of these regions ($R = -.32$, $p = .13$ and $R = -.35$, $p = .11$). However, a correlation with d' was found in the left AG ROI in the strong condition ($R = .53$, $p = .009$). The RSE in AG did not, however, correlate with c ($R = .26$, $p = .23$). The only other retrieval success ROI correlating with d' was the left caudate nucleus ($R = .46$, $p = .03$), but only in the weak condition. Correlations for the strong condition in the AG ROI are plotted in Figure 4A. On the basis of these analyses, the left AG is a $RSA_{d'}$ and candidate memory strength region, and the left and right MFG are RSA_c and candidate response bias regions.

Analysis of Foils in RSA_d'

If differentiation underlies list strength effects, we should see faster onset of information accumulation for strong-list than weak-list foil trials in $RSA_{d'}$. As described earlier, in an information accumulation framework (e.g., diffusion model), stimuli with high-quality evidence accumulate activity toward a decision boundary quicker than stimuli with lower quality evidence. According to differentiation models, strong-list foils have higher-quality evidence (more extreme memory evidence) than weak-list foils, and therefore, strength should affect the rate of increase in activity from trial onset. CRs (not FARs) provide critical evidence of the difference in rate of accumulation because they end at the correct decision boundary, whereas FARs terminate at the wrong decision boundary (and may not follow the expected pattern based on the magnitude of the drift rates).

To evaluate this prediction, we used the Ploran et al. (2007) method, focusing analysis on activity early in the time series, just after trial onset (averaged across Time Points 2 and 3). Ploran et al. (2007) found early differences in the time to reach peak activity (rather than the magnitude of peak activation) for stimuli that were easier to identify in a perceptual task (e.g., provided better evidence). Following their logic, we looked for differences in early activation for strong-list foils that are easier to reject (e.g., provided better evidence). A differentiation account would be supported by strength-based differences in the magnitude

Table 3. ROI Atlas Coordinates and Approximate Anatomic Locations of Retrieval Success Regions and Correlations with d' and c

No.	Hem	Anatomic Location	x	y	z	~BA	#Vox	c-str	c-wk	d'-str	d'-wk
1	L	Post. Cingulate G.	−01	−39	+29	31	306	.18	.17	.32	.21
2	L	Cuneus	−04	−79	+34	19	289	.03	.02	.36	.23
3	R	Mid. Frontal G.	+22	−07	+55	6	191	.27	−.03	−.39	−.24
4	L	Thalamus	−10	−05	+14	NA	141	−.05	.09	−.13	−.09
5	L	Mid. Frontal G.	−24	−03	+55	6	171	.47*	.34	−.32	−.15
6	L	Mid. Frontal G.	−17	+04	+57	6	104	.42*	−.19	−.35	.12
7	L	Precuneus	−13	−68	+52	7	74	.37	.37	.28	−.22
8	L	Thalamus	−03	−17	+11	NA	93	.15	−.02	.15	−.28
9	L	Post. Cingulate G.	−03	−47	+17	30	106	.22	.05	.37	.10
10	L	Angular G.	−42	−70	+37	39	74	.26	.24	.53**	.35
11	L	Caudate	−10	+08	+08	NA	80	−.27	.08	−.21	.46*

Hem = hemisphere; L = left; R = right; G = gyrus; Inf = inferior; Mid = middle; Post = posterior; BA = Brodmann's area; NA = not applicable; #vox = number of voxels in ROI; all locations and Brodmann's areas are approximate. The rightmost four columns are Pearson r values for the parameter (c or d') and RSE for the strong (str) and weak (wk) conditions.
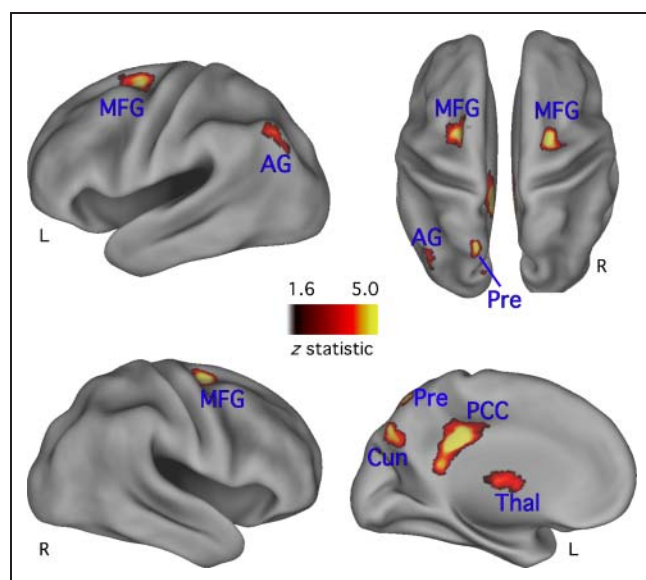
*$p < .05$.

**$p \leq .01$.

of activity at Time Points 2 and 3 (strong-list foil CRs > weak-list foil CRs, indicating a faster approach to peak activation for strong-list foils) in the left AG, the candidate memory strength region. From a diffusion model perspective, the peak magnitudes need not differ; however the rate of accumulation should be faster for strong-list foils. However, t tests
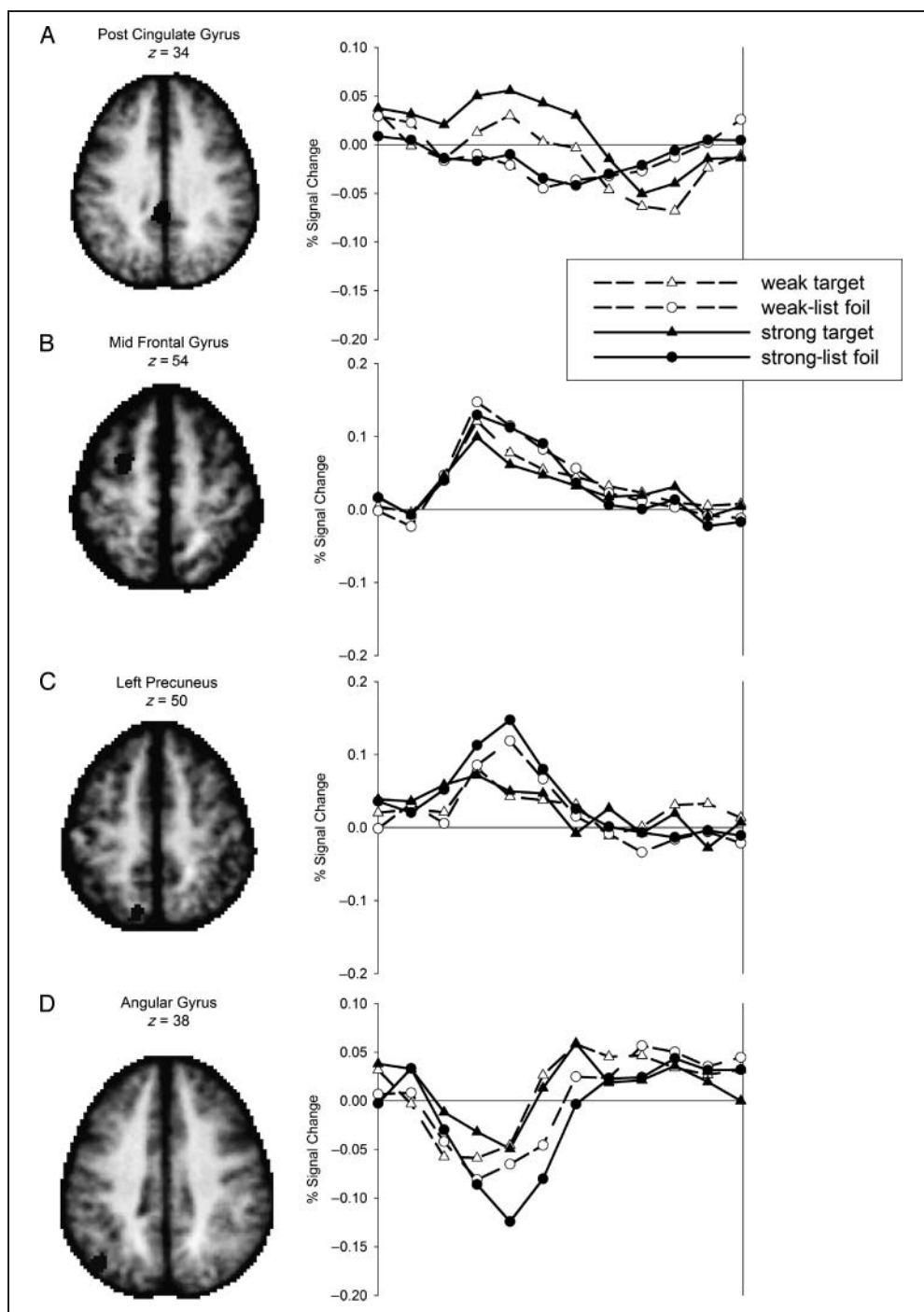

Figure 2. Corrected retrieval success map, projected onto inflated cortical surfaces. Lateral view of the left and right hemispheres are in the first and second row, respectively. Top row right side shows a dorsal view of both hemispheres. Bottom row right side shows a medial view of the left hemisphere. The reliability of activation is indicated by the scale bar, in z score units. L = left; Cun = cuneus; PCC = posterior cingulate cortex; Pre = precuneus; Thal = thalamus.

(one-tailed) revealed no strong > weak differences in the left AG or any other retrieval success ROI (all $p \geq .23$).

Because the most robust memory strength effects are observed in the most confident responses (e.g., see Criss, 2009, 2010), we performed the same analyses using only "sure" trials. Including confidence in the analysis required us to eliminate five participants who lacked a sufficient number of trials in each condition. This analysis revealed a significant early strength effect (strong > weak) on "sure" responses to foils in the left AG ROI, $t(17) = 2.01$, $p = .03$, shown in the left half of Figure 4B ("early"). None of the other retrieval success ROIs approached significance. Peak activity in AG did not differ between conditions, as shown in Figure 4B ("peak"). It should be noted that the "peak" activations in this case are actually well below the baseline. This is true both for Hits and CR (see Figure 3D). This is consistent with our account under the assumption that there is an overall drop in activation in this region during memory task performance; the evidence accumulation process may occur as a positive-going activation on top of this overall drop in activation, or it may occur as a decrease in activity. Although we have stressed the possibility that left AG might profitably be viewed as an evidence accumulator region, with activation increasing as evidence is accumulated, one may also consider the possibility that AG activation might correspond to the total memory activation produced by the stimulus. In this way of thinking, we would expect the BOLD signal strength to be greatest for strong targets, then to decrease for weak targets and weak-list foils, with the lowest signal strength for strong-list foils (as seen in Figure 1, bottom panel). The expected difference between weak-list and strong-list foils is visually

Figure 3. Time courses of the BOLD response for a subset of the RSA. Percent signal change from baseline is plotted over 12 time points from stimulus onset for Post Cingulate Gyrus (A), Mid Frontal Gyrus (B), Left Precuneus (C), and Angular Gyrus (D).

suggestive in left AG (see Figure 3D). However, that difference in the peak the BOLD response is not significant.

Analysis of RSA$_c$

If a criterion shift underlies list strength effects, then we should see different activity for strong-list compared with weak-list foil trials in RSA$_c$ (left and right MFG). Data from each retrieval success ROI were entered into separate mixed effects repeated-measures ANOVA models, with Item Type (correct target, correct foil), Strength (strong, weak), and Time (12 time points) as factors (described in Retrieval Success section). A list strength effect was evaluated using the Strength × Time and Item Type × Strength × Time interaction terms. No interactions of these types were observed in the retrieval success ROIs. Thus RSA$_c$ failed to respond to list strength.

In Analysis of Foils in RSA$_{d'}$ section, we report that five participants were excluded from analyses of "sure" responses to foils because they lacked a sufficient number of such responses. To ensure that these participants did not obscure the analysis just reported, we reran the analysis
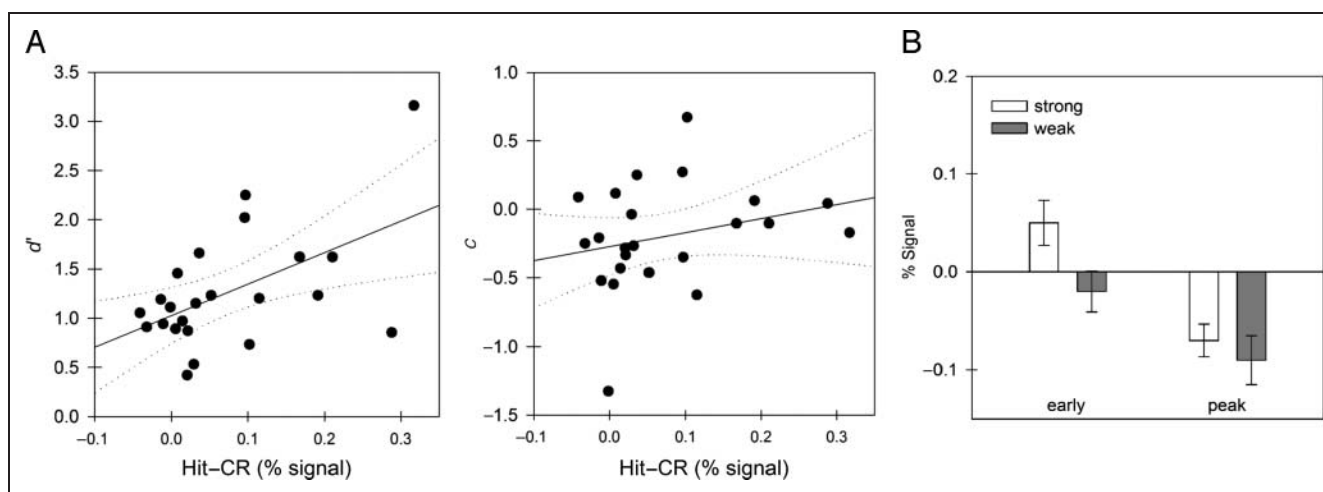
Figure 4. The two panels in Panel A show the correlation between activity in left AG and measures of performance. Discrimination (d'; left) and bias (c; middle) are plotted as a function of RSE (Hit–CR percent signal change) for each individual participant. The RSE is correlated with d' but not c. Panel B shows the magnitude of activation early (averaged over Time Points 2 and 3) and at peak (averaged over Time Points 4, 5, and 6) in AG. Differences between strong-list and weak-list foils early in the time course indicate differences in the rate of evidence accumulation, consistent with differentiation models.

excluding those participants. No interactions were observed. Furthermore, we conducted the ANOVAs separately for "sure" and "maybe" responses and found no interactions. Despite multiple attempts, we found no evidence supporting the hypothesis that RSA_c respond to list strength.

Comparison with O'Connor et al. (2010)

O'Connor et al. (2010) identified a region of left parietal lobe that correlated significantly with bias (c), but not sensitivity (d'). Together with a voxel-based analysis, their findings suggest that the function of the parietal RSA are related more to overcoming response bias than success at retrieval or memory accuracy. To compare our findings with those of O'Connor and colleagues (2010), a 10-mm diameter sphere was created around their peak AG coordinate (Talairach $x, y, z = -42, -50, 41$), after using the nonlinear transformation method developed by Matthew Brett (imaging.mrc-cbu.cam.ac.uk/imaging/MniTalairach) to convert their Montreal Neurological Institute (MNI) coordinates to Talairach atlas space. The resulting ROI, displayed in Figure 5 along with our retrieval success ROIs, is located anterior to our AG RSA_c. Time courses were extracted for Hits and CRs, and correlation analyses were performed. Consistent with the findings of O'Connor et al., we found that the RSE in their ROI correlated positively and reliably with c, but only in the strong condition ($R = 0.42$, $p = .04$; weak: $R = 0.30$, $p = .17$), as shown in Figure 5. There were no correlations with d' for strong ($R = .18$, $p = 42$) or weak ($R = .07$, $p = .76$) conditions.

Exploratory Voxelwise Analysis of the Relationship between the RSE and d' and c

To explore the distribution of voxels sensitive to d' and c, RSE was correlated with d' and c in separate mixed-effects

voxel-by-voxel analyses, with Subject as a random factor. The z-transformed and multiple-comparison corrected images are shown in Figure 6A, overlaid onto an inflated left hemisphere cortical surface. Regions in which activity significantly correlated with d' were found in bilateral MFG near BA 6 and BA 10, left postcentral gyrus, left AG (-36, -70, 39), and bilateral cerebellum (Table 4).

Regions in which activity correlated positively with c included bilateral precentral and postcentral gyrus, bilateral MFG, bilateral cerebellum, right inferior parietal lobe, and right fusiform gyrus (Figure 6A; Table 5). Many of the regions in this map were located in or near structures typically involved in motor planning or execution, including premotor cortex, primary somatosensory/motor cortex, cerebellum, and BG. All regions in the left parietal lobe were located anterior or superior to the lateral parietal regions that correlated with d'. There were very few voxels in which retrieval success activity correlated with both d' and c (Figure 6B, overlap would appear in violet). None of these voxels formed an isolated region, but instead existed at the borders of regions correlating either with d' or c. This observation indicates a sharp distinction between regions involved in signaling successful retrieval and those involved in attentional or strategic demands.

The AG region identified in the exploratory voxelwise correlation analysis was located near the AG retrieval success ROI reported in Table 3. The spatial relationship between these two regions was explored by overlaying them onto an inflated cortical surface. As shown in Figure 6B, there was a high degree of overlap between the ROIs.

DISCUSSION

Differentiation in Episodic Memory

The goal of this article was to use fMRI to evaluate whether differentiation or criterion shifts underlie the SBME in

Figure 5. The ROI derived from O'Connor and colleagues (2010) is shown in green, overlaid with the retrieval success ROIs (red) onto an inflated cortical surface. The bottom row plot d' (left) and c (right) as a function of RSE (HR–CR percent signal change) from the O'Connor ROI. Each data point represents values from a single subject. c but not d' is correlated with RSE in this ROI, replicating the O'Connor et al. finding.
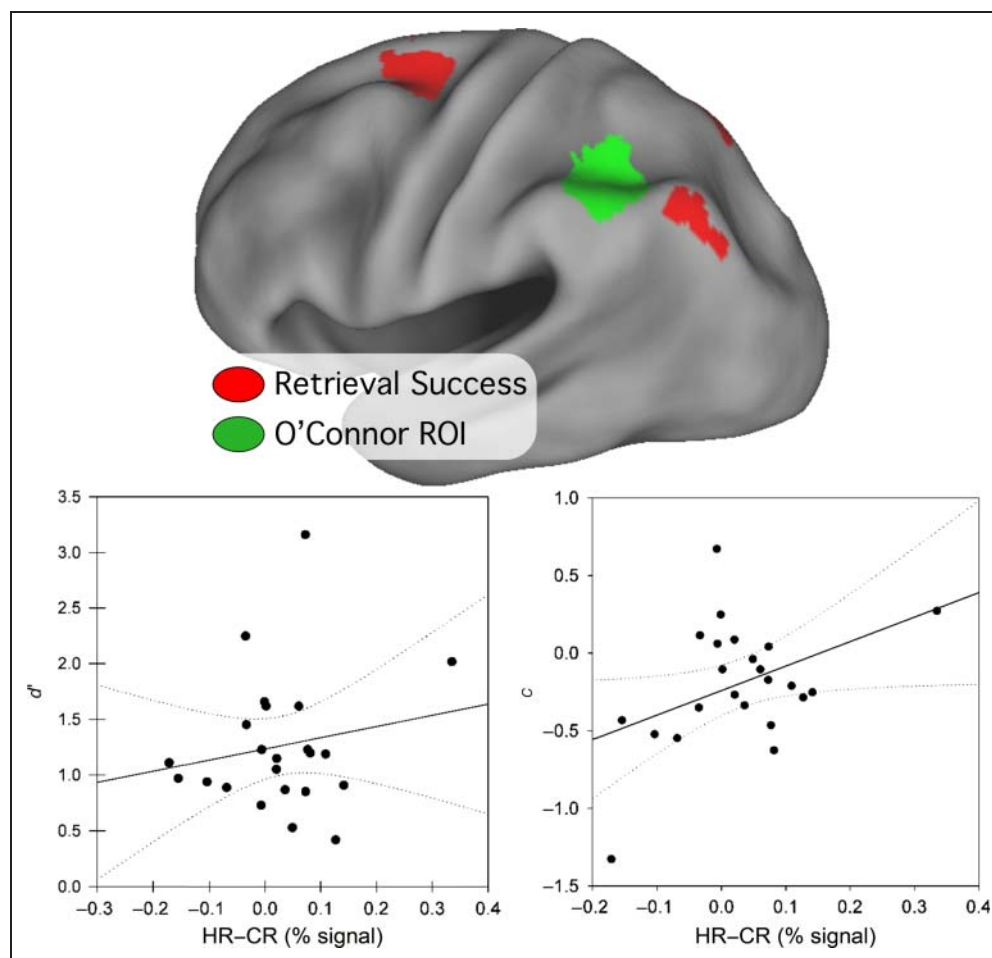
behavioral data. It is of course possible that both differentiation and a criterion shift contribute to the magnitude of the SBME. However, several imaging analyses converged to indicate accumulator-like behavior in or near the AG, supporting a differentiation account. AG showed a Hit–CR difference that grew in magnitude across subjects as d' increased. This region also displayed early differential strength-based effects in the foil conditions, with activity increasing more during the early time points for strong-list foils than weak-list foils on high confidence trials (Figure 4B, "early"). A voxelwise analysis revealed a region in left AG that correlated with d' and that overlapped with the left AG retrieval success ROI (Figure 6B). Finally, AG activity showed no relation to response bias. One interpretation of this set of converging findings is that the left AG serves as one source of information accumulation relevant for a memory decision. However, a conclusive statement about the role of the AG in memory awaits further evidence.

A variety of criterion shift models can mimic predictions from differentiation models (e.g., see Stretch & Wixted, 1998). However, this reasoning fails when faced with the full set of relevant data. Investigations of differentiation with purely behavioral data included an important com- parison condition that is not included here, namely, a condition manipulating the percentage of test trials that are targets. This manipulation is widely regarded as a response bias manipulation. If both paradigms (% target manipulation and SBME) are driven by changes in criterion location, then a similar pattern of behavior should emerge. In a sophisticated analysis of RT distributions (Criss, 2010) and of participant-generated memory strength distributions (Criss, 2009), qualitatively different patterns of results, requiring different model parameters, emerged. Two different processes appear to underlie behavioral performance in the SBME and % target paradigms. Our data cannot evaluate the neural correlates of manipulating target probability. Fortunately, there are two reports measuring fMRI in a % target paradigm discussed in the Response Bias in Anterior and Superior Parietal Lobe section. As a preview, both experiments are consistent with the conclusion we have reached based on the data reported here: Regions sensitive to response bias are not the same as regions sensitive to memory accuracy.

Characterizing neural activation as reflecting memory strength and response bias and especially describing the role of the left AG as reflecting differentiation is a slightly different nomenclature than is typical in the literature.
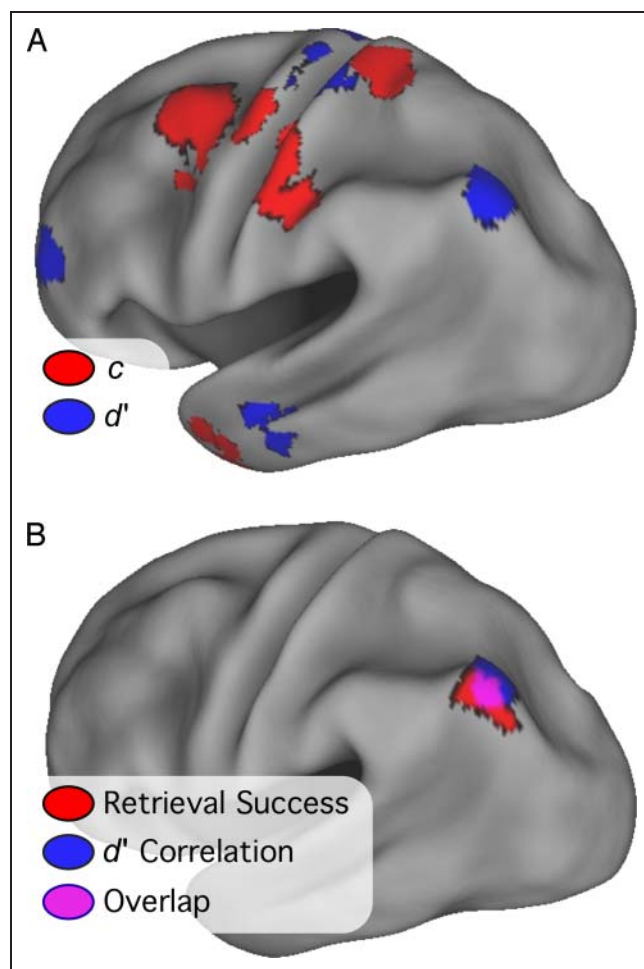
Figure 6. Significant and corrected voxelwise correlations with c (red) and d' (blue) are overlaid onto an inflated cortical surface of the left hemisphere (top). The overlap between activations in or near the AG from the retrieval success (red), d' voxelwise correlation (blue), and analyses is shown in the bottom. Areas of overlap are in violet.

Therefore, the following discussion is aimed at placing our results in the context of prior findings and considering the possibility of reinterpreting prior results.

Memory Retrieval and Left AG

The left parietal cortex, including AG, is frequently reported in fMRI studies of retrieval success (Simons et al., 2008). Activity in some parts of AG tends to decrease below baseline during performance of goal-directed tasks suggesting it is part of the "default mode" network. Using functional connectivity density mapping, Tomasi and Volkow (2011) found that bilateral AG belonged to a default mode network that included the parahippocampal gyrus and medial parietal and frontal cortex.

Analyses of spontaneous low-frequency fluctuations in BOLD fMRI data demonstrate a link between AG and medial-temporal and parietal structures. Nelson and colleagues (2010) used resting state functional connectivity analyses and graph theoretical tools to define a grid

of parietal regions and evaluated RSEs from six studies across regions. Their analyses also categorized the left AG (-45, -67, 36 in MNI-to-Talairach coordinates) with other default mode regions, including the right AG, posterior cingulate, medial and superior frontal, and anterior temporal cortex. Vincent and colleagues used hippocampal ROIs as seed points and found correlated voxels in bilateral AG (Kahn, Andrews-Hanna, Vincent, Snyder, & Buckner, 2008; Vincent et al., 2006).

The AG may temporarily maintain information retrieved from memory as indicated by several studies showing a relationship between the magnitude of signal change and the degree to which retrieval involves recollection. For example, studies using source memory or remember/know (RK) paradigms have been associated with less of a decrease in activity in lateral parietal ROIs near the AG when retrieval involves recollection than when it involves familiarity (Wheeler & Buckner, 2004; Dobbins, Foley, Schacter, & Wagner, 2002; Henson et al., 1999). Two studies using a graded memory strength measure (Montaldi et al., 2006; Yonelinas et al., 2005) found nearby parietal regions (Yonelinas: -33, -56, 36; Montaldi: -39, -68, 39; MNI-to-Talairach coordinates) in which there was less of a decrease in activity as subjective memory strength increased. Vilberg and Rugg (2007) had subjects study pairs of picture stimuli and used a variant of the RK paradigm with two levels of remember response based on amount of recollected information (i.e., with [R2] or without [R1] the studied associate). They found a parietal region near the AG (-39, -77, 40 in MNI-to-Talairach coordinates) that was selective for remember responses and increased activity with amount recollected (R2 > R1). The authors posited that the region operates as an "episodic buffer"

Table 4. List of ROIs with Positive Correlations between RSE and d'

#	Hem	Anatomic Location	x	y	z	~BA	#Vox
1	L	Med. Frontal G.	-07	-24	72	6	196
2	R	Med. Frontal G.	03	50	07	10	152
3	L	Postcentral G.	-29	-28	67	3	169
4	L	Postcentral G.	-06	-41	72	5	141
5	R	Cerebellum	47	-63	-32	NA	222
6	L	Mid. Frontal G.	-38	44	13	10	109
7	L	Mid. Temporal G.	-54	-18	-20	21	106
8	L	Angular G./Precuneus	-36	-70	39	39/19	102
9	R	Cerebellum	05	-25	-34	NA	108
10	L	Cerebellum	-15	-42	-48	NA	133
11	L	Cerebellum	-37	-44	-49	NA	126

Hem = hemisphere; R = right; L = left; Med = medial; Mid = middle; G = gyrus; BA = Brodmann's area; #vox = number of voxels in ROI; all locations and Brodmann's areas are approximate.

Table 5. List of ROIs with Positive Correlations between RSE and C

No.	Hem	Anatomic Location	x	y	z	~BA	#Vox
1	L	Mid. Frontal G.	−34	−00	51	6	287
2	R	Inf. Parietal Lobe	48	−62	43	40	143
3	L	Postcentral G.	−47	−26	38	2	162
4	L	Postcentral G.	−52	−22	51	2	159
5	R	Mid. Frontal G.	48	23	31	9	101
6	R	Mid. Frontal G.	46	11	37	8	135
7	L	Postcentral G.	−31	−21	37	1	116
8	L	Precentral G.	−40	−09	55	6	118
9	L	Cerebellum	−17	−47	−37	NA	141
10	L	Postcentral G.	−21	−39	62	5	204
11	L	Cerebellum	−03	−42	−35	NA	129
12	R	Inf. Temporal G.	40	−05	−40	20	113
13	R	Cerebellum	33	−55	−34	NA	107
14	L	Cerebellum	−33	−41	−42	NA	114
15	R	Cerebellum	26	−41	−32	NA	146
16	R	Mid. Frontal G.	20	−02	52	6	115
17	L	Red Nucleus	−08	−22	−04	NA	101
18	L	Precentral G.	−35	−05	37	6	106
19	L	Pulvinar	−13	−27	06	NA	155
20	L	Precuneus	−12	−62	25	31	119
21	R	Cerebellum	32	−38	−43	NA	108
22	L	Mid. Temporal G.	−47	01	−30	21	157
23	R	Fusiform G.	26	−91	−13	18	158

Hem = hemisphere; L = left; R = right; Inf = inferior; G = gyrus; Mid = middle; BA = Brodmann's area; #vox = number of voxels in ROI; all locations and Brodmann's areas are approximate.

for on-line maintenance of retrieved information. Similarly, Guerin and Miller (2011) found a more ventral left parietal/middle temporal region (−44, −64, 22 in MNI-to-Talairach coordinates) that decreased activity less as more information was retrieved. Although unilateral lesions to the lateral parietal do not affect source recollection of word labels and faces (Simons et al., 2008), there is evidence that bilateral lesions are associated with reduced perceptual detail in recollection (Berryhill, Phuong, Picasso, Cabeza, & Olson, 2007). This inconsistency between lesion and fMRI studies deserves further attention. Collectively these studies have been used to conclude that AG is associated with recollection, and the association with the amount of content precluded a role in memory decisions. However, under an accumulator hypothesis, the amount of content may very well play an important role: The better the evidence for the memory decision, the faster the information ac-

cumulates toward a decision and the faster AG activity changes. In other words, the accumulator hypothesis provides an alternative explanation attributing the role of AG in recollection tasks to high evidence situations.

It has also been proposed that parietal regions play a role in attention to memory. Proposals include the Attention-to-Memory (AtoM; Cabeza, Ciaramelli, Olson, & Moscovitch, 2008; Ciaramelli, Grady, & Moscovitch, 2008) and the Dual-Attentional Processes (Cabeza, 2008) hypotheses. In these accounts, ventral parietal regions mediate reflexive attentional capture of relevant retrieved information whereas dorsal parietal regions are involved in top–down control. In the AtoM framework, the AG is included in the reflexive ventral system and should be more active during target and foil decisions made with high than low confidence because the former items are more salient (Cabeza, 2008). To test whether our findings in AG were consistent with AtoM, we conducted a 2 × 2 ANOVA on the peak estimates from "sure" and "maybe" targets and foils (collapsed over list strength) on the 18 participants with sufficient data. This analysis identified a main effect of Confidence (sure > maybe; $F(1, 17) = 13.87$, $p < .001$) and, as expected due to the region definition procedure, a main effect of Item Type (target > foil) with no interaction ($p = .31$). Thus, consistent with AtoM predictions, activity was greater on "sure" than "maybe" trials for both targets and foils. However, this is also consistent with accumulator activity as described next.

AG Demonstrates Accumulator-like Activity during Episodic Memory

As noted above, the AG region displayed differential strength-based effects early in the time course for foils, suggesting that the momentary signal in this region may be related to the impending memory decision. This finding is similar to the patterns of accumulating activity in a perceptual identification task where participants identify an item that is masked and slowly revealed (Ploran, Tremel, Nelson, & Wheeler, 2011; Wheeler, Petersen, Nelson, Ploran, & Velanova, 2008; Ploran et al., 2007). In those studies, the onset of activity in left parietal cortex ROIs occurred early in the trial and increased at a rate that correlated with the time of identification: Activity increased faster when identification occurred earlier in the trial. The observed patterns of data may reflect an integration-to-bound mechanism (Gold & Shadlen, 2007; Hanes & Schall, 1996) because the information processed was relevant to the decision. That parietal damage does not cause major disruption to memory suggests that the AG is not the sole source of evidence. We note that Ploran et al. (2007) also reported "accumulator-like" regions that decreased rather than increased activity relative to baseline (Figure 3B from that manuscript). Thus, the absolute direction of activity (negative in the AG region reported

here) may be less important than the pattern of accumulation. We also note that their peak voxels (Ploran et al., 2007: −26 −68 38; Ploran et al., 2011: −24, −57, 45 and −24, −71, 34) were ~15 mm closer to the midline of the cerebral hemispheres than the peak voxel in our AG (AG: −42, −70, 37).

In our data, left AG is activated more for correct target than foil trials and more for "sure" than "maybe" trials. This U-shaped function is consistent with findings from several other studies (i.e., Daselaar, Fleck, & Cabeza, 2006; Yonelinas et al., 2005). This is the expected pattern of data obtained when considering SBME data with the diffusion model framework and is consistent with some models of evidence accumulation in macaque LIP (e.g., Mazurek, Roitman, Ditterich, & Shadlen, 2003): Items receive a high-confidence response because they provide high-quality evidence, which has a faster rate of accumulation.

As an alternative to the notion that left AG should be viewed as an evidence accumulator region, we also considered the possibility that left AG activation might correspond to the total memory strength produced by the stimulus. This is consistent with a number of features of the data, including that this is a $RSA_{d'}$. This possibility is also consistent with the finding of Rissman, Greely, and Wagner (2010) that activity in left AG (among other areas) is predictive of subjective memory for items. Under this view, we would expect less activation in AG from strong-list foil CRs than from weak-list foil CRs (as illustrated in Figure 1, bottom panel), and such a trend is visually apparent after onset of the memory probe (Time Points 5 and 6, Figure 3D). However, this finding was not statistically reliable at our estimated peak time of Time Points 4, 5 and 6, and more confident CRs were associated with greater, not less activation that less confident CRs, a finding more consistent with the evidence accumulator hypothesis. The picture presented by the full pattern is tantalizing in suggesting possible roles for both evidence accumulation and total memory activation in the same brain area. We look forward to further investigations that may help clarify the possibly complex role of left AG in recognition memory.

Response Bias in Anterior and Superior Parietal Lobe

Our response bias analyses found parietal regions that were located anterior and superior to the AG regions tracking retrieval success. These included a region (Figure 5) taken from a recent study (O'Connor et al., 2010) reporting a significant correlation with c (but not d') in parietal cortex and regions defined in a voxelwise analysis correlating c with RSE on a subject-by-subject basis (Figure 6A). Somewhat strikingly, the correlation between c and RSE in our estimate of the O'Connor ROI matched very well with the correlation in their ROI, indicating that the finding is reliable across independent studies. Plotting peak coordinates from those studies revealed a section of left lateral parietal

cortex near the AG and supramarginal gyrus that is frequently associated with memory operations (Hit > CR) but rarely reported in studies of attention. Findings from the current study are thus consistent with the claim by O'Connor et al. (2010) that anterior and superior regions of the left parietal cortex are related to strategic attention, but inconsistent in that lateral regions were found to be associated with operations pertaining to the memory decision. O'Connor et al. reported no ROIs where the RSE correlated with d'. The discrepant findings for d' may be related to differences in task or region selection (e.g., the d' and c correlations were conducted on an unpublished data set, not the experiment manipulating cue validity reported in their article).

Our findings are consistent with data reported by Aminoff et al. (2011) and Herron et al. (2004), who manipulated response bias by varying the percent of targets in the test block. In both of these studies and in our data, there is considerable overlap with RSA and regions modulated by response bias. As suggested by O'Connor et al., the term "retrieval success" is perhaps a misnomer as these regions reflect the contribution of both memory retrieval and response bias. Another common finding across these studies is a lack of response bias-dependent activation for left AG. Herron et al. report an RSE but no interaction with response bias for a region near left AG (MNI coordinates −33, −72, 30) and Aminoff et al. do not report a contribution of AG in a regression analysis accounting for their data. Finally, all three studies report many regions of parietal cortex that are modulated by response bias.

Summary

We found evidence suggesting a differentiation account of the SBME, specifically the AG may be accumulating or maintaining accumulated evidence. Furthermore, we found regions whose retrieval success activity correlates with d' and with response bias with few such areas that overlap. However, theories of parietal function in memory are diverse (O'Connor et al., 2010; Cabeza, 2008; Ciaramelli et al., 2008; Vilberg & Rugg, 2008; Wagner et al., 2005; Wheeler & Buckner, 2003), and a definitive statement of the role of the AG in memory awaits further research.

REFERENCES

Aminoff, E., Freeman, S., Clewett, D., Tipper, C., Frithsen, A., Johnson, A., et al. (2011). *Neural correlates of criterion shifting in memory*. Poster presented at the Cognitive Neuroscience Meeting, San Francisco, CA.

Balota, D. A., Yap, M. J., Cortese, M. J., Hutchinson, K. A., Kessler, B., Neely, J. H., et al. (2007). The English lexicon project. *Behavior Research Methods, 39,* 445–459.

Berryhill, M. E., Phuong, L., Picasso, L., Cabeza, R., & Olson, I. R. (2007). Parietal lobe and episodic memory: Bilateral damage causes impaired free recall of autobiographical memories. *Journal of Neuroscience, 27,* 14415–14423.

Buckner, R. L., & Wheeler, M. E. (2001). The cognitive neuroscience of remembering. *Nature Reviews Neuroscience, 2,* 624–634.

Buracas, G. T., & Boynton, G. M. (2002). Efficient design of event-related fMRI experiments using M-sequences. *Neuroimage, 16,* 801–813.

Cabeza, R. (2008). Role of parietal regions in episodic memory retrieval: The dual attentional processes hypothesis. *Neuropsychologia, 46,* 1813–1827.

Cabeza, R., Ciaramelli, E., Olson, I. R., & Moscovitch, M. (2008). The parietal cortex and episodic memory: An attentional account. *Nature Reviews Neuroscience, 9,* 613–625.

Cary, M., & Reder, L. M. (2003). A dual-process account of the list-length and strength-based mirror effects in recognition. *Journal of Memory and Language, 49,* 231–248.

Ciaramelli, E., Grady, C. L., & Moscovitch, M. (2008). Top–down and bottom–up attention to memory: A hypothesis (AtoM) on the role of the posterior parietal cortex in memory retrieval. *Neuropsychologia, 46,* 1828–1851.

Criss, A. H. (2006). The consequences of differentiation in episodic memory: Similarity and the strength based mirror effect. *Journal of Memory and Language, 55,* 461–478.

Criss, A. H. (2009). The distribution of subjective memory strength: List strength and response bias. *Cognitive Psychology, 59,* 297–319.

Criss, A. H. (2010). Differentiation and response bias in episodic memory: Evidence from reaction time distributions. *Journal of Experimental Psychology: Learning, Memory, and Cognition, 36,* 484–499.

Criss, A. H., & McClelland, J. L. (2006). Differentiating the differentiation models: A comparison of the retrieving effectively from memory model (REM) and the subjective likelihood model (SLiM). *Journal of Memory and Language, 55,* 447–460.

Daselaar, S. M., Fleck, M. S., & Cabeza, R. (2006). Triple dissociation in the medial temporal lobes: Recollection, familiarity, and novelty. *Journal of Neurophysiology, 96,* 1902–1911.

Dobbins, I. G., Foley, H., Schacter, D. L., & Wagner, A. D. (2002). Executive control during episodic retrieval: Multiple prefrontal processes subserve source memory. *Neuron, 35,* 989–996.

Fox, M. D., Snyder, A. Z., Barch, D. M., Gusnard, D. A., & Raichle, M. E. (2005). Transient BOLD responses at block transitions. *Neuroimage, 28,* 956–966.

Friston, K., Jezzard, P., & Turner, R. (1994). Analysis of functional MRI time-series. *Human Brain Mapping, 1,* 153–171.

Gold, J. I., & Shadlen, M. N. (2007). The neural basis of decision making. *Annual Review of Neuroscience, 30,* 535–574.

Grill-Spector, K., Henson, R., & Martin, A. (2006). Repetition and the brain: Neural models of stimulus-specific effects. *Trends in Cognitive Sciences, 10,* 14–23.

Guerin, S. A., & Miller, M. B. (2011). Parietal cortex tracks the amount of information retrieved even when it is not the basis of a memory decision. *Neuroimage, 55,* 801–807.

Hanes, D. P., & Schall, J. D. (1996). Neural control of voluntary movement initiation. *Science, 274,* 427–430.

Henson, R. N., Rugg, M. D., Shallice, T., Josephs, O., & Dolan, R. J. (1999). Recollection and familiarity in recognition memory: An event-related functional magnetic resonance imaging study. *Journal of Neuroscience, 19,* 3962–3972.

Herron, J. E., Henson, R. N., & Rugg, M. D. (2004). Probability effects on the neural correlates of retrieval success: An fMRI study. *Neuroimage, 21,* 302–310.

Ho, T. C., Brown, S., & Serences, J. T. (2009). Domain general mechanisms of perceptual decision making in human cortex. *Journal of Neuroscience, 29,* 8675–8687.

Kahn, I., Andrews-Hanna, J. R., Vincent, J. L., Snyder, A. Z., & Buckner, R. L. (2008). Distinct cortical anatomy linked to subregions of the medial temporal lobe revealed by intrinsic functional connectivity. *Journal of Neurophysiology, 100,* 129–139.

Kahn, I., Davachi, L., & Wagner, A. D. (2004). Functional-neuroanatomic correlates of recollection: Implications for models of recognition memory. *Journal of Neuroscience, 24,* 4172–4180.

Konishi, S., Wheeler, M. E., Donaldson, D. I., & Buckner, R. L. (2000). Neural correlates of episodic retrieval success. *Neuroimage, 12,* 276–286.

Kwong, K. K., Belliveau, J. W., Chesler, D. A., Goldberg, I. E., Weisskoff, R. M., Poncelet, B. P., et al. (1992). Dynamic magnetic resonance imaging of human brain activity during primary sensory stimulation. *Proceedings of the National Academy of Sciences, U.S.A., 89,* 5675–5679.

Lancaster, J. L., Glass, T. G., Lankipalli, B. R., Downs, H., Mayberg, H., & Fox, P. T. (1995). A modality-independent approach to spatial normalization of tomographic images of the human brain. *Human Brain Mapping, 3,* 209–223.

Malmberg, K. J. (2008). Recognition memory: A review of the critical findings and an integrated theory for relating them. *Cognitive Psychology, 57,* 335–384.

Mazurek, M. E., Roitman, J. D., Ditterich, J., & Shadlen, M. N. (2003). A role for neural integrators in perceptual decision making. *Cerebral Cortex, 13,* 1257–1269.

McAvoy, M. P., Ollinger, J. M., & Buckner, R. L. (2001). Cluster size thresholds for assessment of significant activation in fMRI. *Neuroimage, 13,* S198.

McClelland, J. L., & Chappell, M. (1998). Familiarity breeds differentiation: A subjective-likelihood approach to the effects of experience in recognition memory. *Psychological Review, 105,* 724–760.

McDermott, K. B., Jones, T. C., Petersen, S. E., Lageman, S. K., & Roediger, H. L., III (2000). Retrieval success is accompanied by enhanced activation in anterior prefrontal cortex during recognition memory: An event-related fMRI study. *Journal of Cognitive Neuroscience, 12,* 965–976.

Michelon, P., Snyder, A. Z., Buckner, R. L., McAvoy, M., & Zacks, J. M. (2003). Neural correlates of incongruous visual information. An event-related fMRI study. *Neuroimage, 19,* 1612–1626.

Miezin, F. M., Maccotta, L., Ollinger, J. M., Petersen, S. E., & Buckner, R. L. (2000). Characterizing the hemodynamic response: Effects of presentation rate, sampling procedure, and the possibility of ordering brain activity based on relative timing. *Neuroimage, 11,* 735–759.

Montaldi, D., Spencer, T. J., Roberts, N., & Mayes, A. R. (2006). The neural system that mediates familiarity memory. *Hippocampus, 16,* 504–520.

Nelson, S. M., Cohen, A. L., Power, J. D., Wig, G. S., Miezin, F. M., Wheeler, M. E., et al. (2010). A parcellation scheme for human left lateral parietal cortex. *Neuron, 67,* 156–170.

Norman, K. A., & O'Reilly, R. C. (2003). Modeling hippocampal and neocortical contributions to recognition memory: A complementary learning systems approach. *Psychological Review, 110,* 611–646.

O'Connor, A. R., Han, S., & Dobbins, I. G. (2010). The inferior parietal lobule and recognition memory: Expectancy violation or successful retrieval? *Journal of Neuroscience, 30,* 2924–2934.

Ogawa, S., Tank, D. W., Menon, R., Ellerman, J. M., Kim, S. G., Merkle, H., et al. (1992). Intrinsic signal changes accompanying sensory stimulation: Functional brain mapping with magnetic resonance imaging. *Proceedings of the National Academy of Sciences, U.S.A., 89,* 5951–5955.

Ojemann, J. G., Akbudak, E., Snyder, A. Z., McKinstry, R. C., Raichle, M. E., & Conturo, T. E. (1997). Anatomic localization and quantitative analysis of gradient refocused echo-planar fMRI susceptibility artifacts. *Neuroimage, 6,* 156–167.

Ollinger, J. M., Shulman, G. L., & Corbetta, M. (2001). Separating processes within a trial in event-related functional MRI I. The method. *Neuroimage, 13,* 210–217.

Ploran, E. J., Nelson, S. M., Velanova, K., Donaldson, D. I., Petersen, S. E., & Wheeler, M. E. (2007). Evidence accumulation and the moment of recognition: Dissociating perceptual recognition processes using fMRI. *Journal of Neuroscience, 27,* 11912–11924.

Ploran, E. J., Tremel, J. J., Nelson, S. M., & Wheeler, M. E. (2011). High quality but limited quantity perceptual evidence produces neural accumulation in frontal and parietal cortex. *Cerebral Cortex, 21,* 2650–2662.

Ratcliff, R. (1978). A theory of memory retrieval. *Psychological Review, 85,* 59–108.

Rissman, J., Greely, H. T., & Wagner, A. D. (2010). Detecting individual memories through the neural decoding of memory states and past experience. *Proceedings of the National Academy of Sciences, U.S.A., 107,* 9849–9854.

Schall, J. D. (2001). Neural basis of deciding, choosing and acting. *Nature Reviews Neuroscience, 2,* 33–42.

Shiffrin, R. M., Ratcliff, R., & Clark, S. E. (1990). List-strength effect: II. Theoretical mechanisms. *Journal of Experimental Psychology: Learning, Memory, and Cognition, 16,* 179–195.

Shiffrin, R. M., & Steyvers, M. (1997). A model for recognition memory: REM-retrieving effectively from memory. *Psychonomic Bulletin & Review, 4,* 145–166.

Simons, J. S., Peers, P. V., Hwang, D. Y., Ally, B. A., Fletcher, P. C., & Budson, A. E. (2008). Is the parietal lobe necessary for recollection in humans? *Neuropsychologia, 46,* 1185–1191.

Snyder, A. Z. (1996). Difference image versus ratio image error function forms in PET-PET realignment. In D. Bailey & T. Jones (Eds.), *Quantification of brain function using PET* (pp. 131–137). San Diego, CA: Academic Press.

Starns, J. J., White, C. N., & Ratcliff, R. (2010). A direct test of the differentiation mechanism: REM, BDCMEM, and the strength-based mirror effect in recognition memory. *Journal of Memory and Language, 63,* 18–34.

Stretch, V., & Wixted, J. T. (1998). On the difference between strength-based and frequency-based mirror effects in recognition memory. *Journal of Experimental Psychology: Learning, Memory, and Cognition, 24,* 1379–1396.

Talairach, J., & Tournoux, P. (1988). Co-planar stereotaxic atlas of the human brain. Thieme, New York.

Tomasi, D., & Volkow, N. D. (2011). Association between functional connectivity hubs and brain networks. *Cerebral Cortex, 21,* 2003–2013.

Van Essen, D. C. (2005). A population-average, landmark- and surface-based (PALS) atlas of human cerebral cortex. *Neuroimage, 28,* 635–662.

Van Essen, D. C., Dickson, J., Harwell, J., Hanlon, D., Anderson, C. H., & Drury, H. A. (2001). An integrated software suite for surface-based analyses of cerebral cortex. *Journal of the American Medical Informatics Association, 41,* 1359–1378. See also brainmap.wustl.edu/caret.

Vilberg, K. L., & Rugg, M. D. (2007). Dissociation of the neural correlates of recognition memory according to familiarity, recollection, and amount of recollected information. *Neuropsychologia, 45,* 2216–2225.

Vilberg, K. L., & Rugg, M. D. (2008). Memory retrieval and the parietal cortex: A review of evidence from a dual-process perspective. *Neuropsychologia, 46,* 1787–1799.

Vincent, J. L., Snyder, A. Z., Fox, M. D., Shannon, B. J., Andrews, J. R., Raichle, M. E., et al. (2006). Coherent spontaneous activity identifies a hippocampal-parietal memory network. *Journal of Neurophysiology, 96,* 3517–3531.

Wagner, A., Shannon, B., Kahn, I., & Buckner, R. L. (2005). Parietal lobe contributions to episodic memory retrieval. *Trends in Cognitive Sciences, 9,* 445–453.

Wheeler, M. E., & Buckner, R. L. (2003). Functional dissociation among components of remembering: Control, perceived oldness, and content. *Journal of Neuroscience, 23,* 3869–3880.

Wheeler, M. E., & Buckner, R. L. (2004). Functional-anatomic correlates of remembering and knowing. *Neuroimage, 21,* 1337–1349.

Wheeler, M. E., Petersen, S. E., Nelson, S. M., Ploran, E. J., & Velanova, K. (2008). Dissociating early and late error signals in perceptual recognition. *Journal of Cognitive Neuroscience, 12,* 2211–2225.

Yonelinas, A. P., Otten, L. J., Shaw, K. N., & Rugg, M. D. (2005). Separating the brain regions involved in recollection and familiarity in recognition memory. *Journal of Neuroscience, 25,* 3002–3008.